

# Raman spectroscopy of optical phonons as a probe of GaN epitaxial layer structural quality

 M.M. Bülbül<sup>1,2,a</sup>, S.R.P. Smith<sup>1</sup>, B. Obradovic<sup>1</sup>, T.S. Cheng<sup>3</sup>, and C.T. Foxon<sup>3</sup>
<sup>1</sup> Department of Physics, University of Essex, Colchester, Essex, CO4 3SQ, UK

<sup>2</sup> Gazi University, Faculty of Arts and Science, Department of Physics, 06500 Teknikokullar, Ankara, Turkey

<sup>3</sup> Department of Physics, University of Nottingham, Nottingham, NG7 2RD, UK

Received 16 July 1999

**Abstract.** We report on Raman scattering measurements of all Raman-active phonons in wurtzite and zinc blende structure GaN epilayers grown on GaAs (001), GaAs (111)A, and GaAs (111)B oriented substrates by means of molecular beam epitaxy (MBE). Raman spectra are taken from these epilayers at room temperature and 77 K in backscattering geometry. The measured values of the phonon frequencies are in agreement with other studies and with lattice dynamic calculations of phonon modes in GaN zinc blende and wurtzite structures. We show that crystal quality is much better in samples grown on GaAs (111) substrates than in samples grown on GaAs (001) substrates. The observation of disorder-activated modes gives information about sample quality. Comparison of the spectra from different thickness epilayers shows that the GaN is more highly disordered close to the substrate, particularly for the (001) substrates.

**PACS.** 78.30.Fs III-V and II-VI semiconductors

## 1 Introduction

The light scattering properties of GaN have received considerable attention. As a nondestructive and noncontact characterisation technique, Raman scattering has been used extensively to study elementary excitations such as phonons and plasmons in GaN samples [1]. From the measured Raman spectra one can obtain information related to the energy and the polarisation properties of the excitations [2]. In addition to the studies of basic properties of the elementary excitations, Raman scattering has also been used to study the material characterisation such as crystal identification, crystal orientation [3, 4], carrier concentration [5], imperfection and strain [6] in GaN to determine the quality of epilayers grown on different substrates and by different methods.

In this work we study the vibrational properties and determine especially the effects of different oriented substrates on quality of crystallisation in GaN thin epilayers of the wurtzite and zinc blende structures on GaAs substrates.

## 2 Experiment

The samples we studied in this work were grown by molecular beam epitaxy (MBE) on semi-insulating GaAs (100),

GaAs (111)A (As-face) and GaAs (111)B (Ga-face) substrates. The growth system is a conventional Varian Mod II MBE system equipped with solid sources of As, Ga, In, Si, Be and Mg. An Oxford Applied Research CARS25 rf-activated plasma source is used as the source of nitrogen, which is initially derived from liquid nitrogen and purified using an active metal getter. The detailed arrangement of the system and growth process has been reported by Foxon *et al.* [7].

Our Raman measurements were carried out at  $T = 300$  K and  $T = 77$  K using the 514.5 nm line of an Ar<sup>+</sup> laser operated at powers of approximately 100–300 mW. The spot size of the laser beam on the sample was about 20  $\mu\text{m}$ . The scattered light was analysed by a Spex double monochromator spectrometer and detected by a standard photon counting technique. Spectra were mainly recorded with a spectral resolution between 2 and 3  $\text{cm}^{-1}$  in the  $z(.,.)\bar{z}$  and  $x(.,.)\bar{x}$  quasi-backscattering configuration where  $z$  is normal to the layers.

## 3 Results and discussion

The zinc blende crystal structure of GaN belongs to the space group F43m ( $T_d^2$ ) with point group symmetry 43m for both atom sites ( $T_d$ ). The only zone-centre phonon modes is of  $T_2$  symmetry which is both IR- and Raman active. The crystal is polar, therefore,  $T_2$  lattice vibrational modes will split into the two components, TO and LO.

<sup>a</sup> e-mail: mahir@quark.fef.gazi.edu.tr

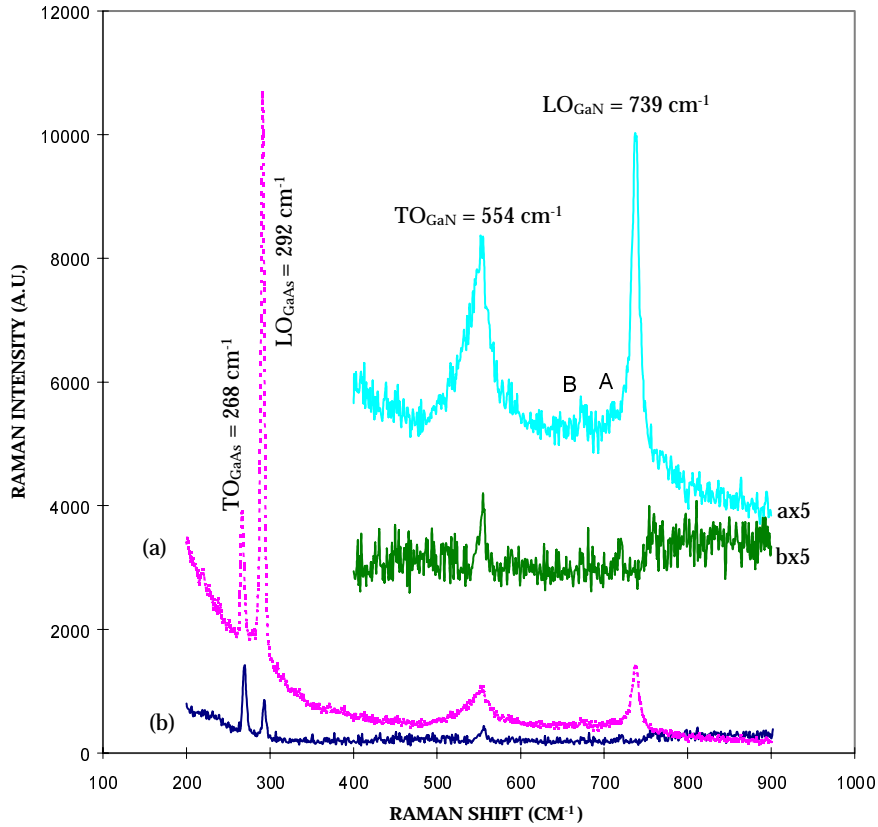


**Fig. 1.** Room temperature Raman scattering spectra from undoped zinc blende GaN on (100)GaAs, MG217, using 514.5 nm laser line: (a) in  $z(xy)\bar{z}$ , (b) in  $z(xx)\bar{z}$  geometries.

The wurtzite structure can be considered to be a slightly modified zinc-blende structure having a small change in the nearest neighbour distance, leading to the energy difference between the Raman modes of these two polytypes. It has two molecular units in the primitive cell that leads to twelve phonon branches. At the centre of the Brillouin zone the acoustic modes comprise the representation

$$1A_1 + 1E_2 \quad (1)$$

and the remaining optical modes include the representations

$$\Gamma_{\text{opt}} = 1A_1 + 2B_1 + 1E_1 + 2E_2. \quad (2)$$

Except for the silent  $B_1$  modes all the other optical modes are Raman active, and the  $A_1$  and  $E_1$  modes are also infrared active for incident radiation with the polarizations  $\mathbf{E} \parallel c$  and  $\mathbf{E} \perp c$ , respectively,  $c$  being the hexagonal axis of the crystal. In a wurtzite crystal, the differences in the  $A_1(z)$  and  $E_1(xy)$  vibrations are caused only due to the small anisotropy in the short range forces, and the LO-TO splitting caused by the long-range electrostatic forces in  $\alpha$ -GaN is much larger than the  $A_1$ - $E_1$  splitting due to the anisotropy in the short-range interatomic forces [8].

In Figure 1 we show typical room temperature Raman spectra from undoped cubic GaN, MG217 ( $d = 0.8 \mu\text{m}$ ), grown on GaAs (100). The spectra were taken in  $z(xy)\bar{z}$  and  $z(xx)\bar{z}$  backscattering geometries. As it is clearly

seen, the GaN epilayers are so transparent that they allow substrate phonon modes to appear in the spectrum. The GaN optical phonon region is well-separated from that of the GaAs substrate. Therefore the spectra can be investigated and easily distinguishable from each other. We may divide the spectrum into two parts. The first part between  $100\text{--}400 \text{ cm}^{-1}$  belongs to the GaAs substrate and the second part beyond  $400 \text{ cm}^{-1}$  belongs to the GaN phonon modes region. The peaks at  $269 \text{ cm}^{-1}$  and  $292 \text{ cm}^{-1}$  are respectively the TO and LO phonon modes of the GaAs substrate [9]. According to the selection rules for zinc blende structure, the TO phonon mode at  $269 \text{ cm}^{-1}$  is forbidden in  $z(xy)\bar{z}$  backscattering geometry. However it can appear relatively weakly due to specular reflections in the interface region and to the incident and scattered light not being perpendicular to the crystal surface. In  $z(xx)\bar{z}$  geometry, both TO and LO phonon modes are forbidden; however they appear feebly also due to the above reasons.

In the GaN region, we see two noticeable peaks at  $554 \text{ cm}^{-1}$  and  $739 \text{ cm}^{-1}$ . The allowed LO phonon mode at  $739 \text{ cm}^{-1}$  is expected, but not the TO phonon mode at  $554 \text{ cm}^{-1}$  in this geometry as in the GaAs substrate region. This forbidden band becomes allowed due to the three effects that modify strict backscattering selection rules: (1) reflection from the substrate in the epilayer allows forward as well as backward scattering in GaN. Forward scattering permits the TO phonon to be seen; (2) deviation of incident and scattered angle from  $90^\circ$ .

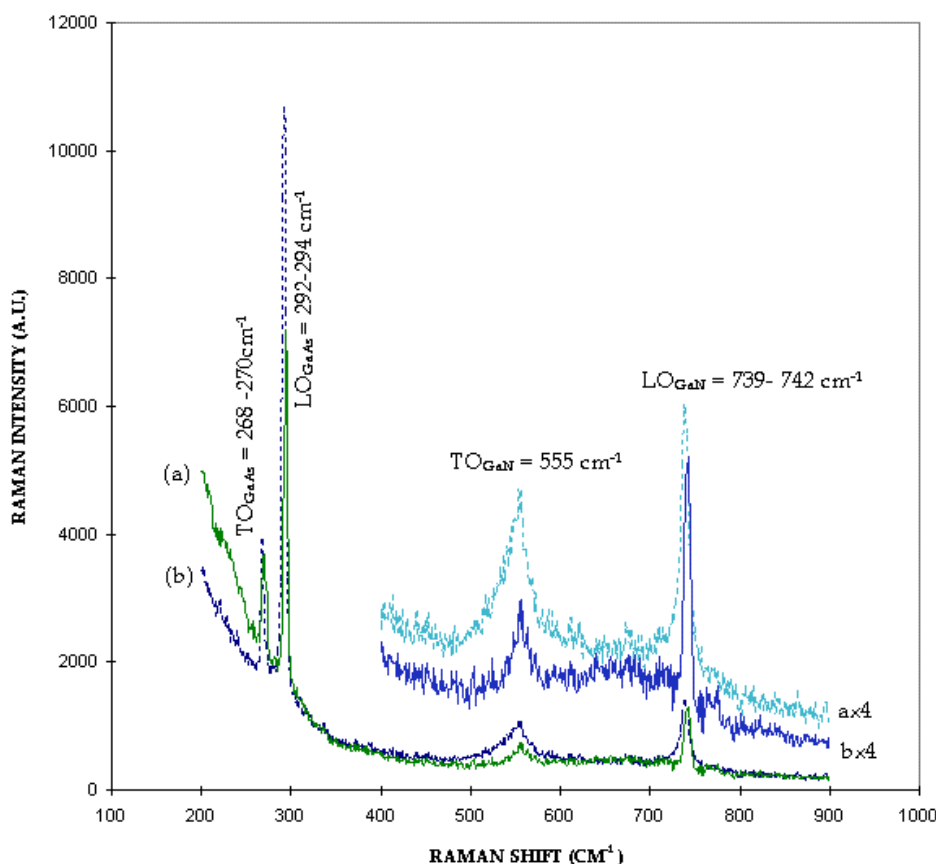


**Fig. 2.** Room temperature (a) and 77 K (b) Raman scattering spectra from cubic GaN/GaAs(001), MG217, using 514.5 nm laser line in  $z(x, -)\bar{z}$  configuration.

Although the incident external angle is  $\sim 60^\circ$  the internal angle is much closer to normal incidence (less than  $10^\circ$ ). This allows some TO scattering, but is not very significant; (3) specular reflection at the interface in effect removes the polarisation selection rules for scattering in both the epilayer and substrate. Regarding these effects (1) is clearly important leading to the very strong GaN TO. The contributions of (2) and (3) are less significant.

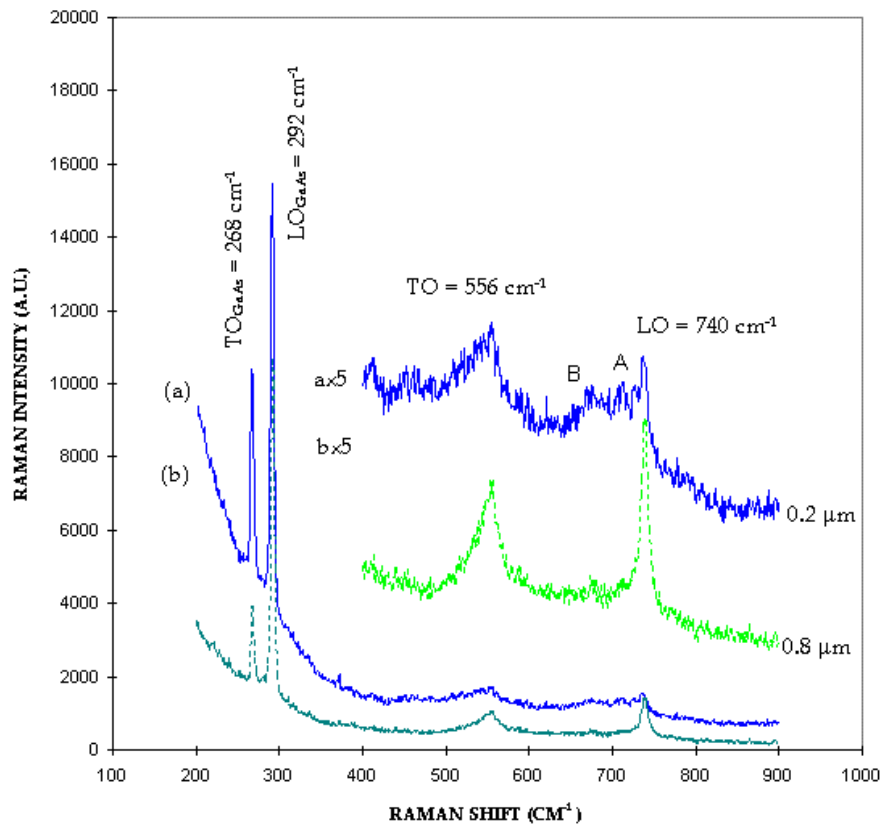
In Figure 2, Raman spectra from the zinc-blende sample MG217, taken at room temperature and 77 K, are seen. At 77 K, the LO mode at  $739\text{ cm}^{-1}$  shifts  $3\text{ cm}^{-1}$  higher to  $742\text{ cm}^{-1}$ , the TO mode at  $554\text{ cm}^{-1}$  remains almost unchanged. Full-width at half maximum (FWHM) of the LO phonon mode decreases from  $10\text{ cm}^{-1}$  to  $6\text{ cm}^{-1}$ . In the spectrum two subsidiary peaks A and B at  $710\text{ cm}^{-1}$  and  $676\text{ cm}^{-1}$ , respectively, occur at the low energy side of LO phonon mode. The latter was also observed by infrared measurements and interpreted as arising from a relatively highly disordered region of thickness about 15 nm at the interface between the GaN and the substrate [10].

The peaks A and B have also been observed in other Raman measurements [5,11]. We propose that the peak A at  $710\text{ cm}^{-1}$  is probably due to a two phonon summation band originating from the combination of L-point LA and TO phonons. Zi *et al.* [12] have made first-principles calculations of the phonon dispersion curves for GaN, and quote the frequencies of these modes as  $144$  and  $569\text{ cm}^{-1}$

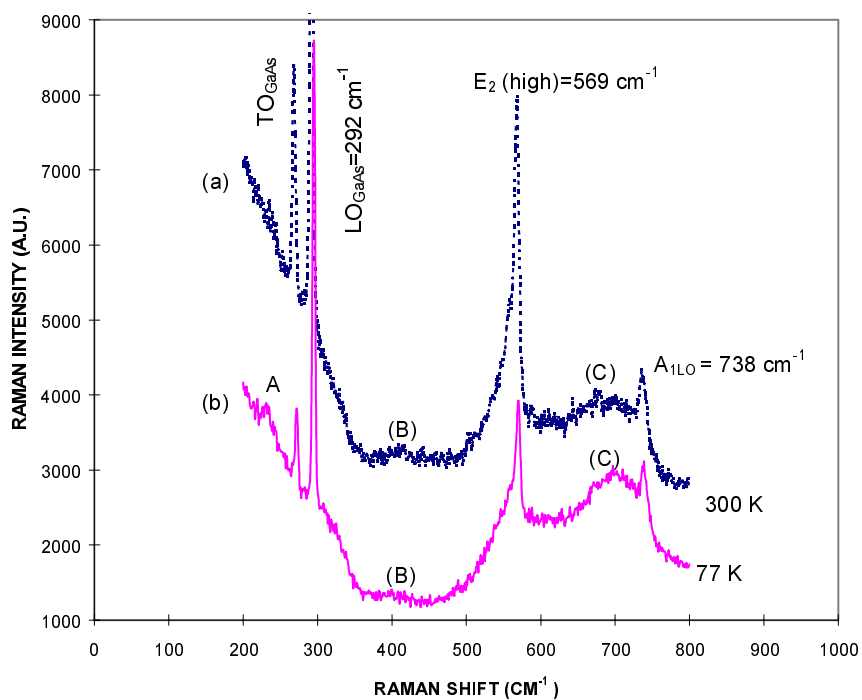
respectively (obtained by analysis of experimental data on the closely-related hexagonal structure). These values give a combination band at  $713\text{ cm}^{-1}$ , in close correspondence with our observed frequency of  $710\text{ cm}^{-1}$ . However, it is curious that this band was not observed in Raman scattering of hexagonal GaN.

Figure 3 compares the spectra of zinc-blende samples of different epilayer thicknesses ( $0.2\text{ }\mu\text{m}$  and  $0.8\text{ }\mu\text{m}$ ). The thicker sample shows comparatively sharp LO and TO phonon peaks, with little other structure, whilst disorder-activated structure (peaks A and B) are clearly visible in the thinner sample. It is apparent that the average crystal quality is superior in the thicker sample, and that the region close to the substrate is highly disordered.

The remaining spectra concern wurtzite GaN. In Figure 4 we show typical room temperature and 77 K Raman spectra of the  $\alpha$ -GaN on GaAs (100), from the sample MG159 in  $z(x, -)\bar{z}$  geometry. In the GaN region, the two peaks at  $569\text{ cm}^{-1}$  and  $738\text{ cm}^{-1}$  are attributed to  $E_2(\text{high})$  and  $A_1(\text{LO})$  modes, respectively, which are allowed in the  $z(x, -)\bar{z}$  configuration. The broad band between  $E_2$  and  $A_1(\text{LO})$ , which is localised at about  $670\text{ cm}^{-1}$ , arises from disordered-activated scattering, which permits the observation of phonon modes over the whole Brillouin Zone with no wavevector selection rule  $q \approx 0$ . This band is also observed by some authors in GaN epilayers grown by MBE [9,11]. The increase



**Fig. 3.** Room temperature Raman scattering spectra from undoped zinc blende GaN on GaAs (100), (a) MG107 ( $d = 0.2 \mu\text{m}$ ) and (b) MG217, ( $d = 0.8 \mu\text{m}$ ) using 514.5 nm laser line in  $z(xy)\bar{z}$  geometry.



**Fig. 4.** Room and liquid nitrogen temperature Raman spectra from wurtzite GaN on GaAs (001), MG159, using 514.5 nm  $\text{Ar}^+$  laser line in  $z(x, -)z$  configuration.

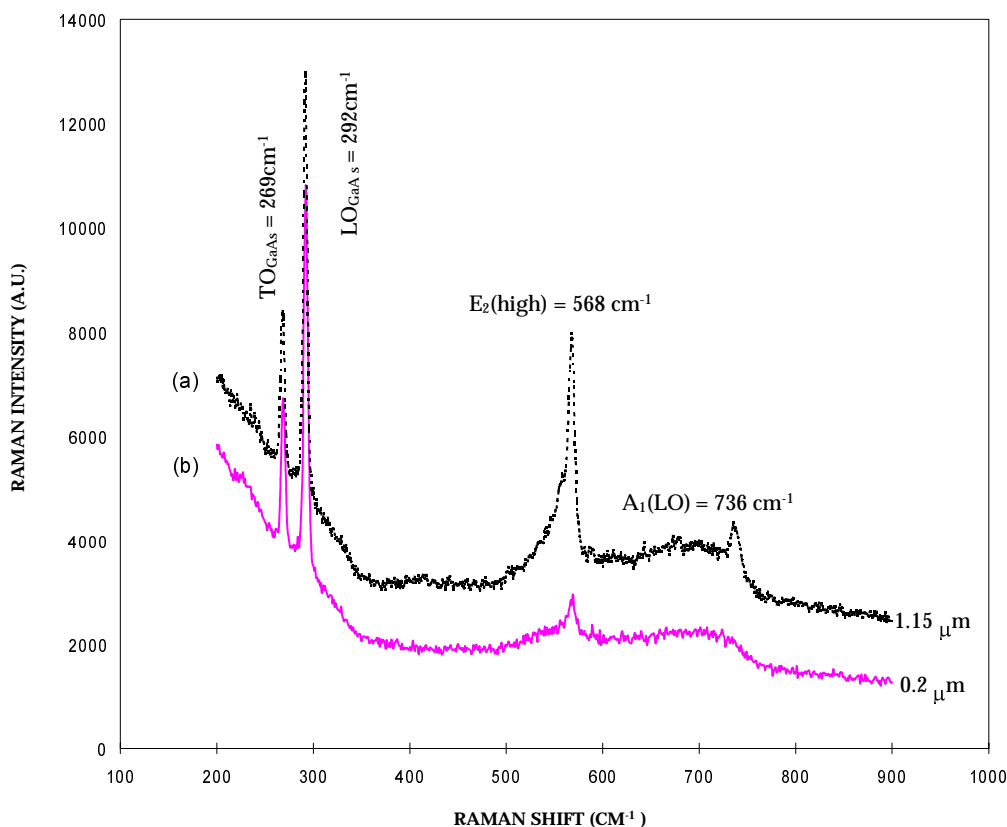


**Fig. 5.** Room temperature Raman spectra from undoped wurtzite GaN on GaAs (001), (a) MG159 ( $d = 1.15 \mu\text{m}$ ) and (b) MG142 ( $d = 0.2 \mu\text{m}$ ), using 514.5 nm laser line in  $z(x, -)\bar{z}$  configuration.

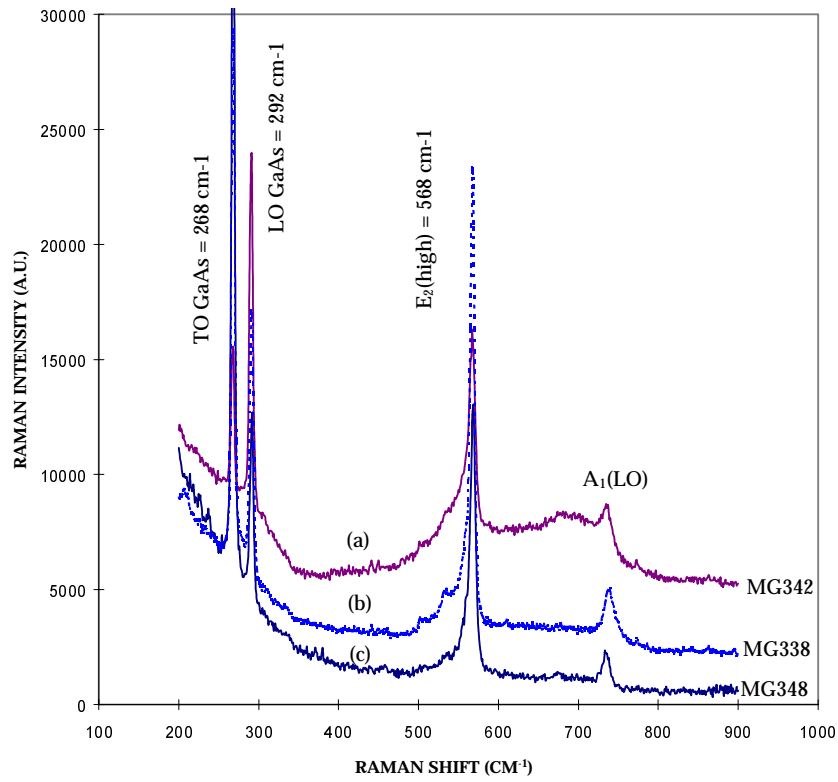
in disorder increases the intensity of the disorder-activated LO (DALO) phonon scattering around  $670 \text{ cm}^{-1}$ . At the same time, the scattering from the  $A_1(\text{LO})$  ( $q = 0$ ) mode decreases in intensity. In all cases where disorder-activated modes are observed, there are in addition other broad features in the spectrum that cannot be assigned to modes originating from specific parts of the Brillouin zone. It is noticeable that 77 K spectrum usually shows a stronger disorder-activated spectrum than at room temperature. This may be due to the fact that, on cooling, increase in the penetration depth allows more scattering from the more highly disordered region near the substrate, and perhaps also an increase in thermal stresses in this region.

Figure 5 gives the phonon intensities depending on the sample thickness. The quality of the spectra (as determined by the ratio of  $q = 0$  modes to disorder-activated modes) is clearly better for the thicker sample. In Figure 5b Raman spectrum from the sample with thickness  $0.2 \mu\text{m}$ , MG142, is shown. In this comparatively thin sample, we were able to detect only the  $E_2$  mode at  $568 \text{ cm}^{-1}$  and no  $A_1(\text{LO})$  phonon mode.

Figure 6 shows the comparison of Raman spectra from three samples; (a) MG342 grown on GaAs (001), (b) MG338 grown on GaAs (111)B substrates and (c) MG348 grown on GaAs (111)A, which were grown under the same growth conditions. As we see from the figure, the spectrum of sample MG338 on GaAs (111)B is much better than those of sample MG342 on GaAs (001) and

MG348 grown on GaAs (111)A substrates. The following points should be noted:

- (i) The DALO peak A at about  $670 \text{ cm}^{-1}$  in the sample MG342 on GaAs (001), completely disappeared from the spectrum of sample MG338 on GaAs (111). This peak has been observed by many authors in both wurtzite and cubic GaN epilayers as we pointed out above. Its absence in the (111) samples indicates improved sample quality. Low temperature photoluminescence (PL) spectrum and some other structural properties of such films, assessed using X-ray, transmission electron microscopy (TEM) and infrared spectroscopy, have been published elsewhere [10,13].
- (ii) The phonon peaks in sample MG338 on GaAs (111)B are noticeably more symmetric than that of MG342 on GaAs (001).
- (iii) The linewidth ( $\Gamma$ ) of the  $E_2(\text{high})$  mode is about  $7.5 \text{ cm}^{-1}$  in sample MG338 on GaAs (111)B and  $\Gamma = 10 \text{ cm}^{-1}$  in MG342 on GaAs (001). This also indicates improved sample quality.
- (iv) The value of the  $A_1(\text{LO})$  phonon mode in sample MG338 is  $3 \text{ cm}^{-1}$  higher than that in MG342. In general, the frequency of the  $A_1(\text{LO})$  mode decreases slightly with increasing epilayer thickness. Presuming that the internal strain also decreases with increasing thickness, it appears that, despite their superior quality, the epilayers on GaAs(111) may be more strained than that of the epilayers on GaAs(100).



**Fig. 6.** Room temperature Raman spectra from three wurtzite GaN epilayers: (a) MG342/GaAs (001); (b) MG338/GaAs (111)B and (c) MG348/GaAs(111)A using 514.5 nm line of Ar<sup>+</sup> laser in  $z(x, -)\bar{z}$  geometry.

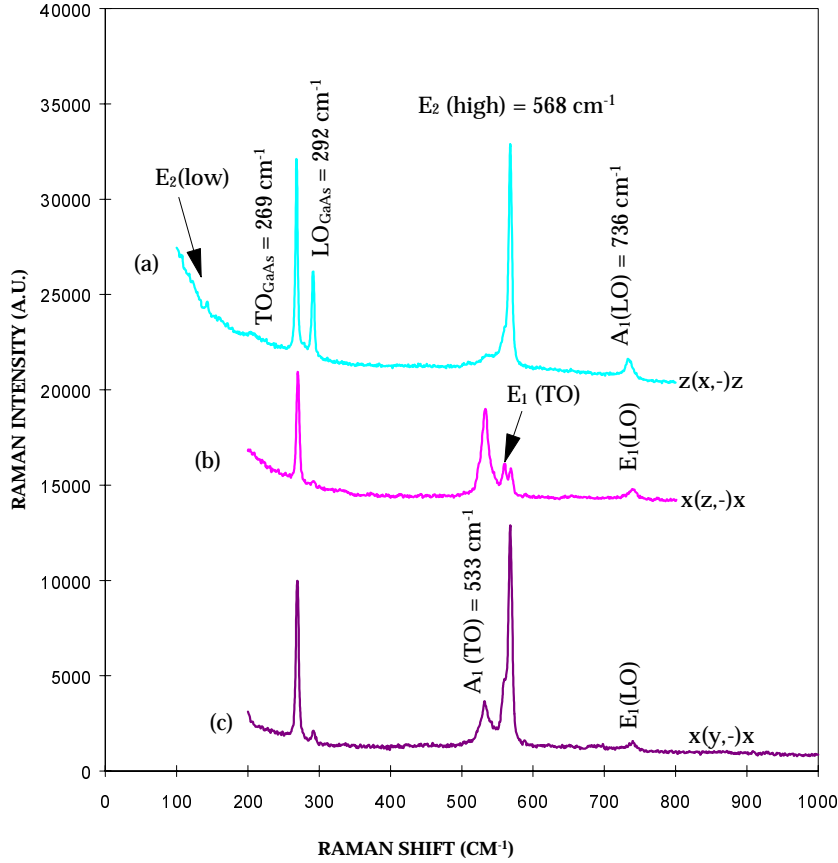


**Fig. 7.** Room temperature Raman spectra from lightly p-type Mg-doped  $\alpha$ -GaN/GaAs (111)B, MG526, using 514.5 nm laser line in different configurations.

In Figure 7 we have determined all of the symmetry-allowed Raman-active optical phonon frequencies using a high quality wurtzite structure GaN epilayer.

## 4 Conclusion

In this work, we have shown that Raman spectroscopy is a very useful technique for obtaining spectra giving important information on characterisation and vibrational properties of III–V semiconductor GaN epilayers

We have characterised and compared the zinc-blende and wurtzite polytypes of GaN epilayers, which can be distinguished by the different modes and selection rules for first-order Raman scattering. We have observed all of the symmetry-allowed Raman-active optical phonon frequencies for both zinc blende and wurtzite structures. For zinc blende structure, the assigned values of the TO and LO phonon modes are  $554\text{ cm}^{-1}$  and  $739\text{ cm}^{-1}$ , respectively. These values are in good agreement with other experimental works by Raman, infrared measurements and also theoretical calculations. We observed the effects of sample thicknesses and temperature on the sample crystallisation.

In the wurtzite structure GaN epilayers with different thickness, the frequency value of the  $E_2(\text{high})$  phonon mode were the same. On the other hand, the  $A_1(\text{LO})$  phonon mode in thin epilayers grown on GaAs (001) surface was slightly higher than that in thicker samples, probably due to the effect of stress relaxation in the thicker samples but perhaps also due to differences in growth conditions. Moreover we have shown the effect of different substrate orientations on this mode. The epilayers grown on a GaAs (111) surface exhibit much sharper and more symmetric phonon profiles as well as a lower intensity of disorder-activated modes, indicating higher quality structure. However, the frequency value of the  $A_1(\text{LO})$  phonon modes is noticeably ( $3\text{ cm}^{-1}$ ) higher than that of an otherwise GaN layer grown on (001) surface, indicating the existence of stress due to lattice mismatch between epilayer and substrate in spite of good crystallisation.

M.M.B. wishes to thank Gazi University in Turkey for research leave and financial support during his work in U.K.

## References

1. T. Kozawa, T.Kachi, H. Kano, Y. Taga, M. Hashimoto, N. Koide, K. Manabe, *J. Appl. Phys.* **75**, 1098 (1994).
2. O. Briot, B. Gil, M. Tchounkeu, R.L. Aulombard, F. Demangeot, J. Frandon, M. Renucci, *J. Electron. Mater.* **26**, 294 (1997).
3. H. Siegle, L. Eckey, A. Hoffmann, C. Thomsen, B.K. Meyer, D.Schikora, M. Hankenl, K. Lischka, *Solid State Commun.* **96**, 943 (1995).
4. H. Siegle, P. Thurian, L. Eckey, A. Hoffman, C. Thomsen, B.K. Meyer, H. Amano, I. Akasaki, T. Detchprohm, K. Hiramatsu, *Appl. Phys. Lett.* **68**, 1265 (1996).
5. P. Perlin, C. Jauberthie, J. P. Itie, S. A. Miquel, I. Grzegory, A. Polian, *Phys. Rev. B* **45**, 83 (1992).
6. W. Rieger, T. Metzger, H. Angerer, R. Dimitrov. O. Ambacher, M. Stutzmann, *Appl. Phys. Lett.* **68**, 970 (1996).
7. C.T. Foxon, T.S. Cheng., S.V. Novikov, D.E. Lacklison, L.C. Jenkins, D. Johnston, J.W. Orton, S.E. Hooper, N. Baba-Ali, T.L. Tansley, V.V. Tret'yakov, *J. Cryst. Growth* **150**, 892 (1995).
8. C.A. Argulleo, D.L. Rousseau, S.P.S. Porto, *Phys. Rev.* **181**, 1351 (1969).
9. C. Patel, T.J. Parker, H. Jamshidi, W.F. Sherman, *Phys. Stat. Solidi B* **122**, 461 (1984).
10. G. Mirjalili, T.J. Parker, S.F. Shayesteh, M.M. Bülbül, S.P.R. Smith, T.S. Cheng, C.T. Foxon, *Phys. Rev. B* **57**, 4656 (1998).
11. A. Tabata, R. Enderlein, J.R. Leite, S.W. da Silva, J.C. Galzerani, D. Schikora, M. Kloidt, K. Lischka, *J. Appl. Phys.* **79**, 4137 (1996).
12. J. Zi, W. Guanghong, Z. Kaiming, X. Xide, *J. Phys. Cond. Matter.* **8**, 6323 (1996).
13. T.S. Cheng, C.T. Foxon, N.J. Jeffs, O.H. Hughes, B.G. Ren, Y. Xin, P.D. Brown, C.J. Humphreys, A.V. Andranov, D.E. Lacklison, J.W. Orton, M. Halliwell, *MRS Internet J. Nitride Semiconductor Research* **1** (1996), article 32.